ELSEVIER

Polymer Vol. 37 No. 1, pp. 125–135, 1996

0032-3861/96/$15.00+0.00

Thermodynamics of solubilization of functional copolymers in the grafted shell of core–shell impact modifiers: 2. Experimental

M. Lu, H. Keskkula and D. R. Paul*
Department of Chemical Engineering and Center for Polymer Research, The University of Texas at Austin, Austin, TX 78712, USA
(Received 19 April 1995; revised 14 June 1995)

Certain styrene/maleic anhydride copolymers (SMA) are completely miscible with poly(methyl methacrylate) (PMMA). This paper explores the solubilization of SMA copolymers in the grafted PMMA shell layer of emulsion-made core–shell impact modifiers by examining glass transition behaviour and morphology of SMA/core–shell modifier blends. There appears to be a single, composition-dependent hard phase T_g for these blends at all compositions by dynamic mechanical analysis. Transmission electron microscopy reveals that SMA copolymers are evenly distributed around the core–shell particles. Neither approach was able to determine the upper solubilization limit expected from theoretical considerations. A blend of core–shell modifier with polystyrene (PS), which is not miscible with PMMA, was also examined for comparison.

(Keywords: styrene/maleic anhydride copolymers; poly(methyl methacrylate); core–shell impact modifiers)

INTRODUCTION

The first paper in this series[1] developed a simple thermodynamic theory for examining the extent to which free chains (type B) can be solubilized into a 'brush' of grafted chains (type A) that form the shell of core–shell impact modifiers. The degree of solubilization is affected by the interaction energy between polymer chains of types A and B, the molecular weight and the conformational size of polymers A and B, and the grafting density or the thickness of the shell layer. The main driving force for mixing is a favourable interaction between polymer chains A and B, while conformational issues associated with dissolving one polymer in the restricted space of a graft layer or brush provide significant barriers to solubilization. In general, this theory predicts that solubilization is favoured when the B chains are small and the A chains are large and initially exist in a thin shell layer.

Interest in this solubilization process was stimulated by observations that styrene/maleic anhydride copolymers (SMA) can be useful in dispersing emulsion-made core–shell impact modifiers into nylon 6[2]. The modifiers of interest have a thin shell layer of poly(methyl methacrylate) (PMMA) chains grafted to a rubber core. Earlier studies[3] have shown PMMA to be miscible with certain SMA copolymers, which suggests that SMA copolymers might be solubilized into this PMMA shell. Of course, anhydride units readily react with amine chains ends of polyamides. This combination of physical and chemical interaction has been proposed to contribute to the ability of small amounts of SMA to facilitate the dispersion of these impact modifier particles into nylon 6[2]. Rheological changes associated with the grafting of nylon 6 to SMA also promote the dispersion process[4].

In this paper, experimental studies were carried out to provide more direct evidence of the solubilization of SMA copolymers (polymer B) in the grafted PMMA (polymer A) shell layer by examining glass transition behaviour and morphology of SMA/core–shell modifier blends. If the SMA copolymer is solubilized into the PMMA shell, the hard phase glass transition temperature should follow the behaviour for miscible SMA/PMMA blends. On the other hand, if all of the SMA copolymer is not solubilized into the PMMA shell, a separate SMA phase should form leading to two hard phase glass transition temperatures and a level of phase separation that perhaps can be detected by electron microscopy.

EXPERIMENTAL

Materials

Two core–shell impact modifiers from Rohm and Haas Co. were used in this work. Paraloid EXL3300 (EXL3300) has an n-butyl acrylate based rubber core grafted with a PMMA ($\bar{M}_n = 80\,000$) hard shell with a particle diameter of 3300 Å. Paraloid EXL3607 (EXL3607) has a butadiene based rubber core grafted with a PMMA ($\bar{M}_n = 80\,000$) shell with a particle diameter of 1800 Å. The PMMA shell comprises 20% of the total mass for both types of modifiers. Further details about these materials are given elsewhere[5,6].

The two random styrene/maleic anhydride copolymers used are commercial products of Arco Chemical Co.

* To whom correspondence should be addressed

They contained 8 and 14% maleic anhydride by weight and are designated as SMA8 (Dylark 232) with $\bar{M}_n = 100\,000$ and $\bar{M}_w = 200\,000$ and SMA14 (Dylark 332) with $\bar{M}_n = 90\,000$ and $\bar{M}_w = 180\,000$, respectively.

The poly(methyl methacrylate), Plexiglass V811, from Rohm and Haas Co., had $\bar{M}_n = 52\,900$ and $\bar{M}_w = 105\,400$. The polystyrene was from Fina Chemical Co. and has $\bar{M}_n = 100\,000$ and $\bar{M}_w = 350\,000$.

Procedures

All the blends were made by melt mixing in a Killion single-screw extruder ($L/D = 30$, 2.54 cm screw diameter) at 40 rev min^{-1}. The temperature of extrusion was set at 240°C for SMA/core–shell blends and at 200°C for SMA/PMMA blends, since lower critical solution temperature behaviour for SMA8/PMMA blends has been reported at slightly above 200°C[3]. Samples for dynamic mechanical analysis were prepared by compression moulding pelletized extrudates at 160–170°C.

A Perkin–Elmer DCS 7 was used to measure the glass transition behaviour of SMA/PMMA blends at a scan rate of 20°C min^{-1} (second heats were recorded). The glass transition temperatures were taken as the midpoint of the transition.

Since the PMMA shell layer comprises only 20% by weight of these modifiers, differential scanning calorimetry (d.c.s.) techniques are not sensitive enough for detecting the hard phase glass transition. Dynamic mechanical thermal analysis (d.m.t.a.) was employed to analyse the glass transition properties of the blends containing the core–shell impact modifiers. The moulded samples were cut into specimens measuring approximately $3 \times 12 \times 20$ mm and tested using a Polymer Laboratories' dynamic mechanical thermal analyser, DMTA, at a frequency of 1 Hz and a heating rate of 5°C min^{-1} in the single-cantilever bending mode. The glass transition temperature can be defined by the location of either the tan δ or the loss modulus, E'', peak.

The morphology of selected blends was examined by transmission electron microscopy (TEM) using a Jeol SEM 200CX. Ultrathin sections were obtained by microtoming compression moulded specimens using a Riechert-Jung ultramicrotome at −80°C which were then stained with OsO_4 vapour for at least 30 min or with RuO_4 vapour for a maximum of 15 min.

GLASS TRANSITION BEHAVIOUR

In this section, the glass transition behaviour of SMA/PMMA binary blends will be compared with that of SMA/core–shell modifier blends. The core–shell materials, of course, exhibit glass transitions characteristic of the PMMA shell and the rubbery core. The primary focus here is on the hard phase glass transition temperature (T_g), to seek evidence of whether (a) the SMA mixes with the PMMA chains of the shell to produce a single T_g (like that shown for SMA/PMMA binary blends), (b) the SMA and the PMMA exist in separate phases such that two glass transitions characteristic of these materials are observed, or (c) some intermediate situation exists. The glass transition of the rubber phase of the core–shell particles is affected slightly by blending with SMA owing to internal stress effects like those noted in similar systems[7–10].

SMA/PMMA blends

The glass transition behaviour of PMMA blends with SMA8 and SMA14 were measured by both d.s.c. and d.m.t.a. *Figure 1* shows the T_g determined by d.s.c. as a function of blend composition. For both SMA copolymers, a single, composition-dependent T_g is observed, indicating complete miscibility of SMA8 or SMA14 with PMMA as previously reported.[3] The solid lines were drawn to best represent the experimental data points, while the dashed lines were calculated from the Fox equation[11]

$$\frac{1}{T_g} = \frac{W_{PMMA}}{(T_g)_{PMMA}} + \frac{W_{SMA}}{(T_g)_{SMA}} \quad (1)$$

where W represents the weight fraction. For both blend

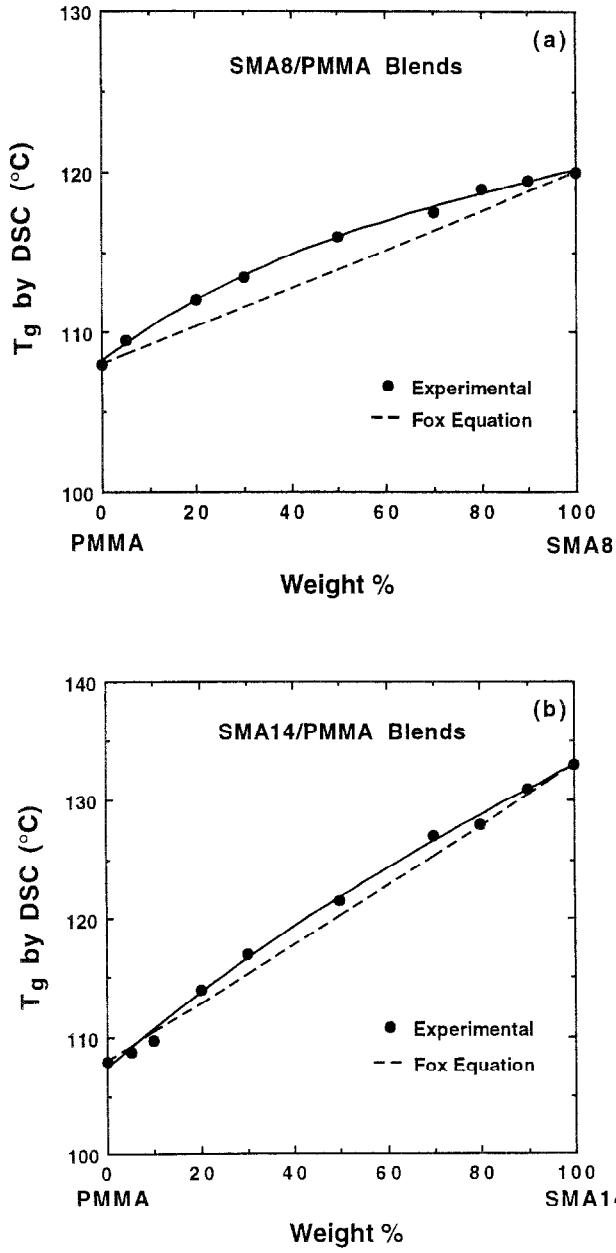

Figure 1 Glass transition behaviour of PMMA blends with (a) SMA8 and (b) SMA14, determined by d.s.c. at 20°C min^{-1}. The dashed lines were calculated from the Fox equation by using the two extreme points

systems, the d.s.c. measurements deviate positively from additivity or the prediction of the Fox equation. Such curvature is not common for blends but has been reported for a number of systems[12–18]. Such behaviour has been attributed to highly favourable interchain interactions[17,18], excess entropy of mixing effects[14,15], or loss of free volume on mixing[19–21]. Establishing the reason for this behaviour in the present case is beyond the scope of this investigation.

Figure 2 shows the dynamic mechanical properties of SMA8 as a function of temperature which is typical of results for PMMA and for SMA/PMMA blends. The storage modulus E' decreases steeply at the glass transition temperature while the loss modulus E'' and tan δ both show a peak in the temperature region of this transition. However, the peak temperature from the loss modulus E'' curve is 11–12°C lower than that from the tan δ curve. This offset in peak temperatures can be explained in terms of the rapid decrease in storage modulus (E') with temperature at T_g shown by amorphous polymers[22,23]. Recall that tan δ is related to the real and loss moduli by

$$\tan \delta = E''/E' \quad (2)$$

The large decrease in real modulus at the glass transition temperature causes the tan δ peak to occur at a higher temperature than observed for the E'' curve. It has been suggested[22] that the E'' curve may be more suitable for judging the glass transition temperature for amorphous materials, such as SMA copolymers or their blends with PMMA, which have a very rapid drop in storage modulus associated with this transition.

Figure 3a shows the glass transition temperatures of SMA8/PMMA blends, as defined by the peak in the E'' curves, as a function of the SMA weight fraction. The peak temperatures from the tan δ curves are shown in *Figure 3b*. The results from the E'' curves deviate positively from additivity and the Fox equation, as observed from the d.s.c. measurements (see *Figure 1*); whereas the results from the tan δ curves deviate negatively from the Fox prediction. The latter values are usually about 10 to 15°C higher than those determined from the E'' curves.

Figure 4 shows corresponding results for PMMA blends with SMA14; the trends are generally similar to those shown for SMA8 blends in *Figure 3*. The differences in curvature seen for the two measures of T_g by dynamic mechanical behaviour need to be remembered when these results are compared with similar results for SMA/core–shell modifier blends in the next sub-section. Generally, the peak temperatures from E'' curves give a better representation of the glass transition temperature.

SMA/core–shell modifier blends

Figure 5 shows dynamic mechanical properties for several blends of the core–shell impact modifier, EXL3300, with SMA8 as a function of temperature. The decrease in storage modulus at the glass transition of the rubbery phase is less than one decade for each composition. On the other hand, there is a decrease of about two decades in real modulus associated with the glass transition of the grafted PMMA and there is a corresponding large peak in the tan δ curve. In general, one might expect a larger decrease in real modulus at the glass transition of the rubbery phase than at that of the shell phase, since there is only 20% of the grafted PMMA shell. However, because the shell is the continuous phase in this case, the rigidity of the sample is determined mainly by the shell phase[24]. The loss modulus E'' does not show such a large peak at the glass transition of the shell layer. Since the storage modulus E'

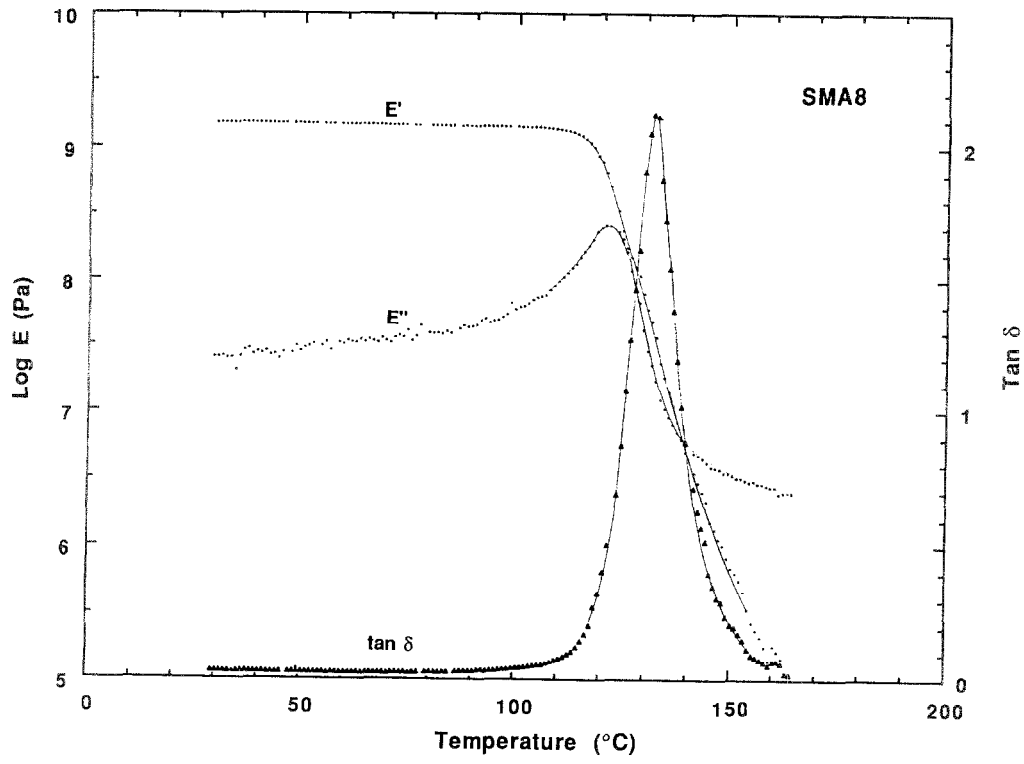

Figure 2 Dynamic mechanical properties of SMA8 as a function of temperature

shows only a small drop at the glass transition of the rubber phase, the tan δ peak occurs at approximately the same temperature as the E'' peak. As SMA8 is added, the drop in storage modulus and the size of the tan δ peak associated with the rubber phase glass transition decrease in magnitude as would be expected, see *Figure 5*, and occur at a slightly lower temperature as explained later. In contrast, the decrease in storage modulus and the size of the tan δ peak associated with the hard phase transition become larger and shift progressively to higher temperatures on addition of the SMA8. The latter changes seem to occur over a single temperature interval which suggests that the hard phase is composed of a mixture of the grafted PMMA and the SMA8, rather than separate PMMA and SMA phases.

Figure 6 shows the peak temperatures from E'' and tan δ curves for the hard phase of SMA8/EXL3300 blends as a function of the SMA8 weight fraction of the hard phase, i.e. $W_{SMA8}/(W_{SMA8} + W_{PMMA})$; the mass of PMMA, or W_{PMMA}, is 20% of the mass of the core–shell material in the blend. The solid lines were drawn to represent the experimental results while the dashed lines were calculated from the Fox equation by using the two extreme points. The peak temperatures from the tan δ curves are 10–15°C higher than those from the E'' curves; however, in both cases, the experimental measurements deviate positively from the Fox prediction, similar to the d.s.c. observation for the SMA8/PMMA binary blends. The important point from the perspective of the current objective is that there seems to be only one hard phase T_g that shifts with composition smoothly between the limits of the two pure hard

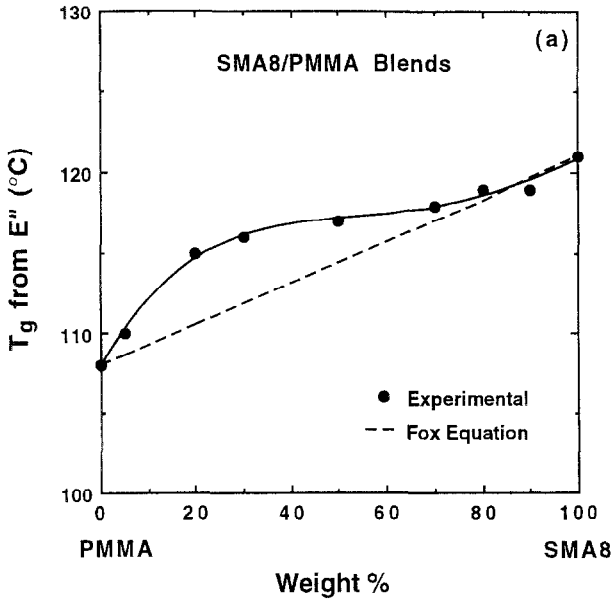

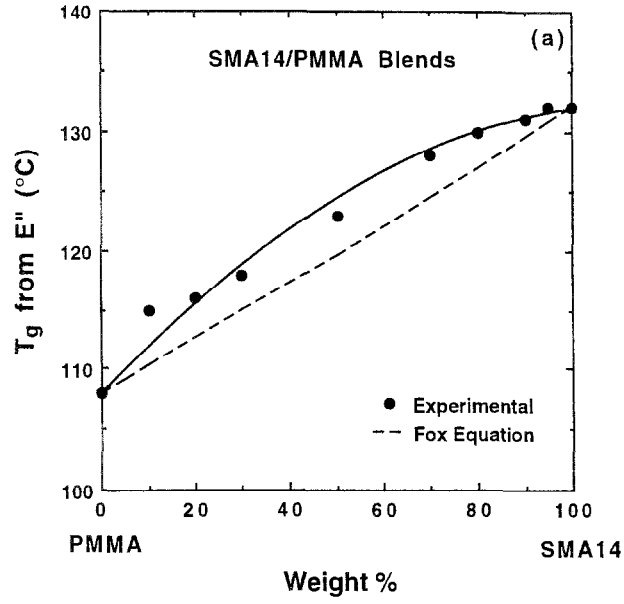

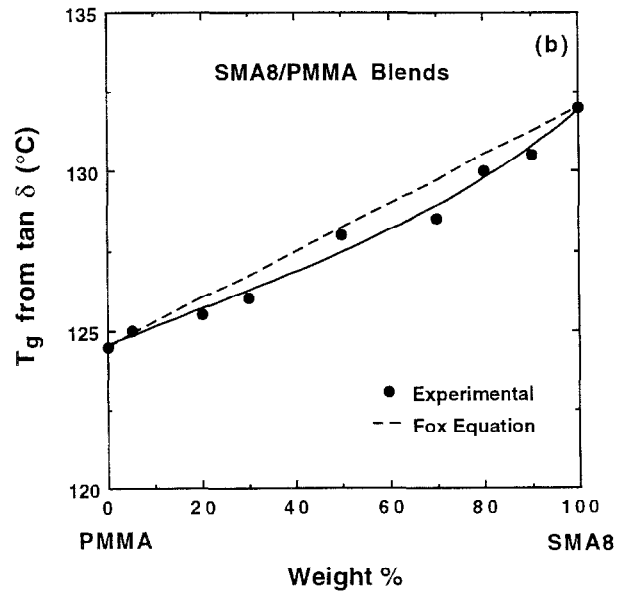

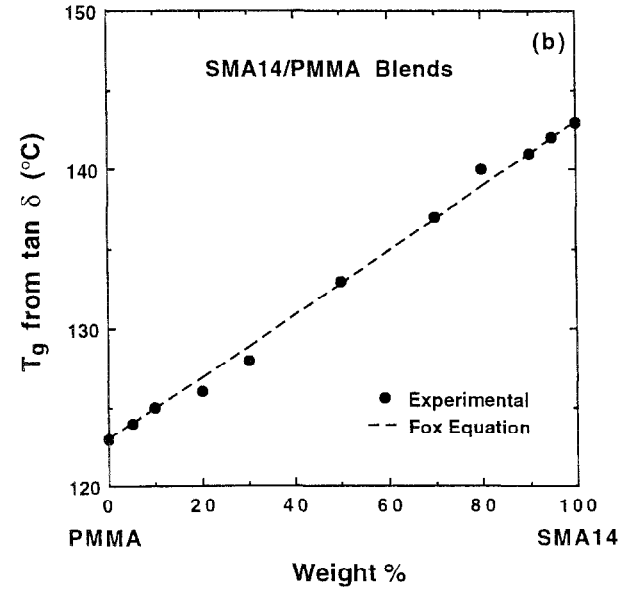

Figure 3 Glass transition temperature defined by the maximum of (a) loss modulus E'' and (b) tan δ curves for SMA8/PMMA blends as a function of SMA8 fraction. The dashed lines were calculated from the Fox equation by using the two extreme points

Figure 4 Glass transition temperature defined by the maximum of (a) loss modulus E'' and (b) tan δ curves for SMA14/PMMA blends as a function of SMA14 fraction. The dashed lines were calculated from the Fox equation by using the two extreme points

components, SMA8 and PMMA. This suggests there is complete solubilization of SMA8 in the grafted PMMA shell of the impact modifier particles. A similar trend is observed for the SMA14/EXL3300 blends as seen in *Figure 7*. The fact that the curvature of the tan δ peak temperatures for SMA blends with the core–shell materials is opposite to that with PMMA reflects subtle differences in how E' changes with temperature in the two cases and does not seem germane to the overall conclusion.

The above results seem to imply that there is no limit to how much SMA8 and SMA14 can be solubilized in the PMMA grafted layer of the core–shell particle. However, the thermodynamic theory developed in the

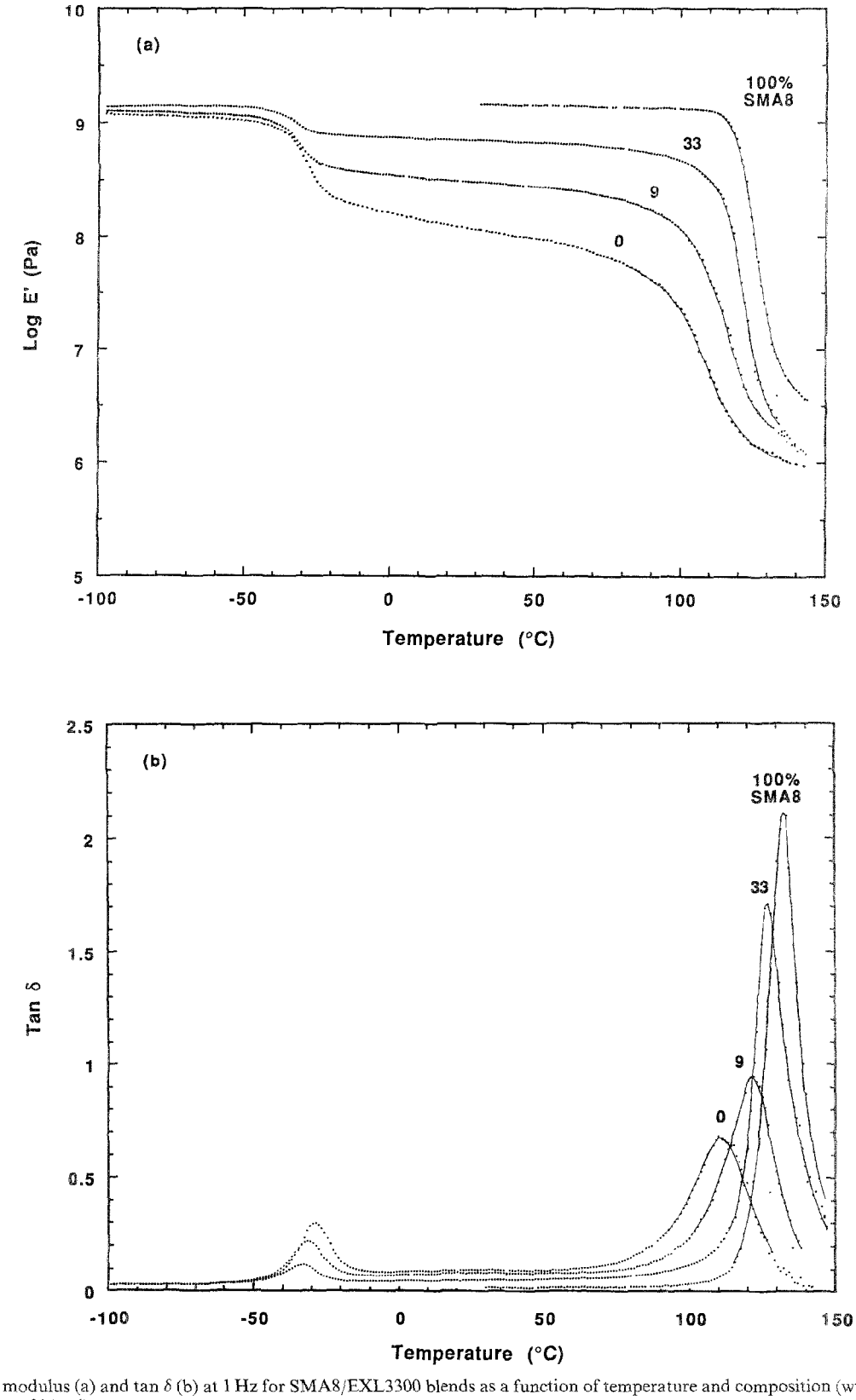

Figure 5 Storage modulus (a) and tan δ (b) at 1 Hz for SMA8/EXL3300 blends as a function of temperature and composition (wt% SMA8 shown is based on total mass of blend)

preceding paper[1] clearly indicates that there must be some limit to the amounts of SMA8 or SMA14 that can be solubilized in a grafted PMMA brush. Simple geometrical considerations lead to a similar conclusion as discussed later.

Broadening of the glass transition region has been interpreted in terms of short-range compositional fluctuations in miscible blends of free chains[25] and in terms of longer range composition gradients for mixtures within microdomains of block copolymers[26,27]. It is useful to consider the current results from the latter point of view. Here, the breadth of the T_g region from dynamic mechanical analysis is defined as the width of the tan δ peak at half its height. *Figure 8* shows this measure of T_g breadth for SMA8/PMMA and SMA8/EXL3300 blends as a function of the SMA8 fraction. Tie lines connecting the composition extremes are shown for reference. It is noted that the transition breadths for blends based on the core–shell modifier are always somewhat larger than those for blends with PMMA. The same trend is seen in *Figure 9* for the SMA14 based blends. The geometrical constraints imposed by having one end of the PMMA chains grafted to the rubber core while the other end is free ensure that there must be some concentration gradient of any SMA solubilized within this very thin shell layer as has been argued for mixing of polymer chains within the microdomains in a block copolymer[26,27].

As mentioned earlier, the tan δ peak in *Figure 5* associated with the glass transition of the rubber core shifts slightly to lower temperatures as SMA8 is added. This is shown in *Figure 10*, where the rubber peak

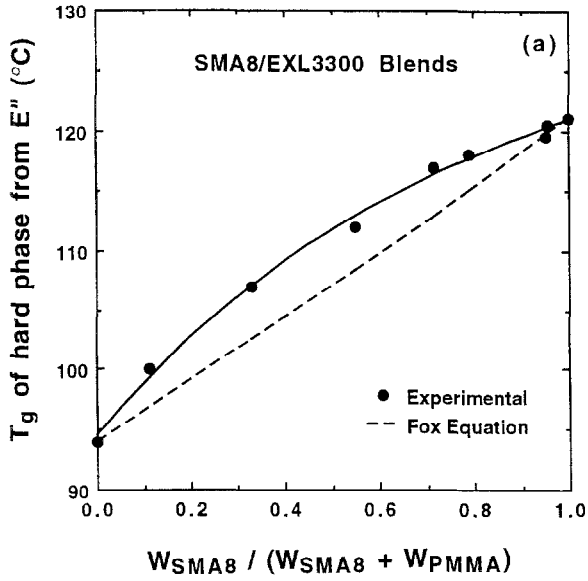

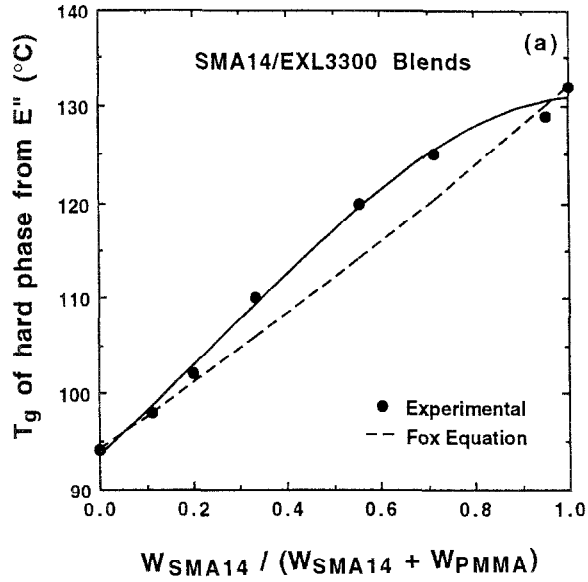

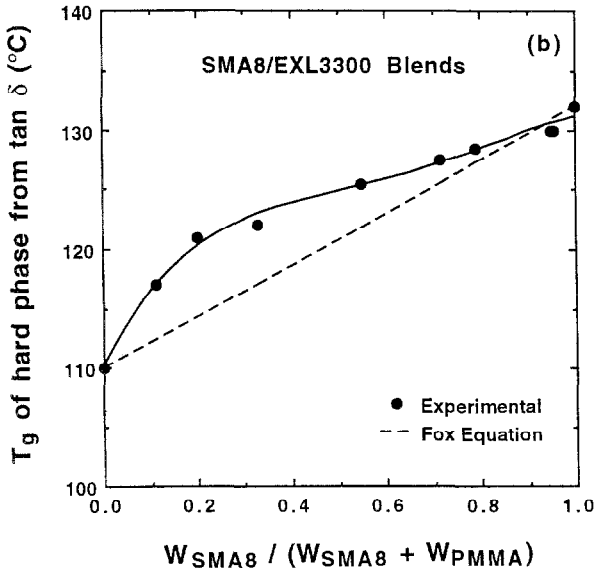

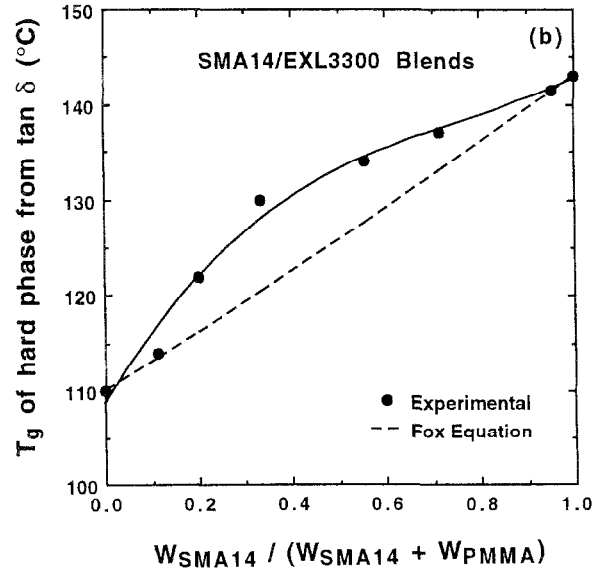

Figure 6 Glass transition temperature of hard phase defined by the maximum of (a) loss modulus E'' and (b) tan δ curves for SMA8/EXL3300 blends as a function of SMA8 fraction in hard phase. The dashed lines were calculated from the Fox equation by using the two extreme points

Figure 7 Glass transition temperature of hard phase defined by the maximum of (a) loss modulus E'' and (b) tan δ curves for SMA14/EXL3300 blends as a function of SMA14 fraction in hard phase. The dashed lines were calculated from the Fox equation by using the two extreme points

temperature is plotted as a function of the weight fraction of the SMA copolymer added on a rubber-free basis. That addition of SMA8 or SMA14 lowers the glass transition temperature of the rubber phase is entirely consistent with previous studies[7–10]. This effect is believed to be caused by a negative pressure created by the difference in thermal expansion coefficients of the soft and hard phases[10]. It is also of interest to note that the addition of SMA14 leads to a slightly larger drop than SMA8. This may reflect a different level interaction with the PMMA and, hence, solubilization. SMA14 is expected to have a more favourable interaction with PMMA than SMA8[3,28].

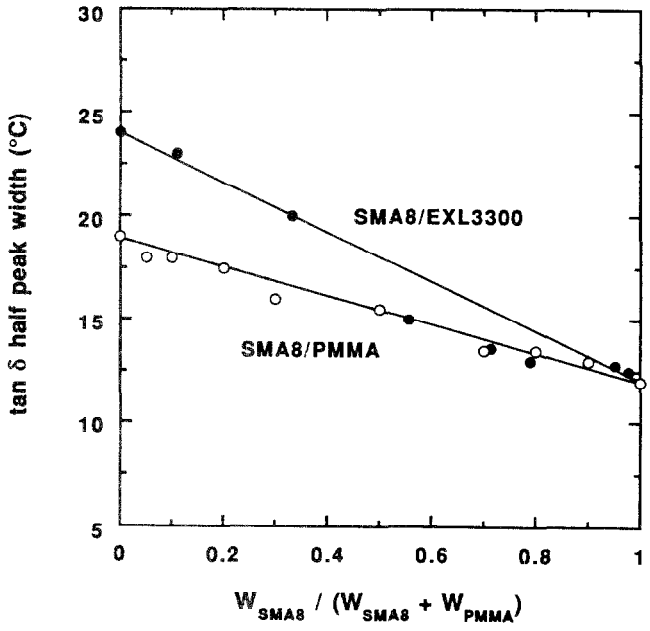

Figure 8 Width of the tan δ peak at half-height for the hard phase glass transition *versus* weight fraction of SMA8 in hard phase for SMA8/PMMA and SMA8/EXL3300 blends

MORPHOLOGY

In principle, examination of the morphology of blends of a core–shell impact modifier with a polymer, like SMA, at high magnification by transmission electron microscopy (TEM) should provide some information about whether the added polymer is solubilized into the shell or forms a separate phase, particularly if the domains of the separate phase are large relative to the size of the emulsion particles. On this basis, such blends were examined by TEM techniques. Before examining these results it is useful to consider what one might expect to see.

If the added polymer and the shell of the impact modifier particle have no affinity for each other or are very incompatible, one would expect that a blend containing a small amount of the modifier could show large aggregates of modifier particles since it would be difficult to disperse them individually in such a matrix. However, good dispersion in this case does not confirm solubilization since this could result from the PMMA shell being wetted by the matrix, as is the case when polycarbonate is the matrix[29–32]. A blend containing a large volume of the impact modifier relative to the added polymer might be expected to reveal large domains relative to the emulsion particles of the latter in a matrix formed by the impact modifier. However, the relative size of these domains would clearly depend on the degree of incompatibility, the mixing process, and the rheological properties of the components. *Figure 11* attempts to show what one might expect to observe by TEM if solubilization (or very intimate dispersion) of the added polymer did occur. First of all, it is important to recognize that a melt processed collection of core–shell particles, without any additive, would not form a fully

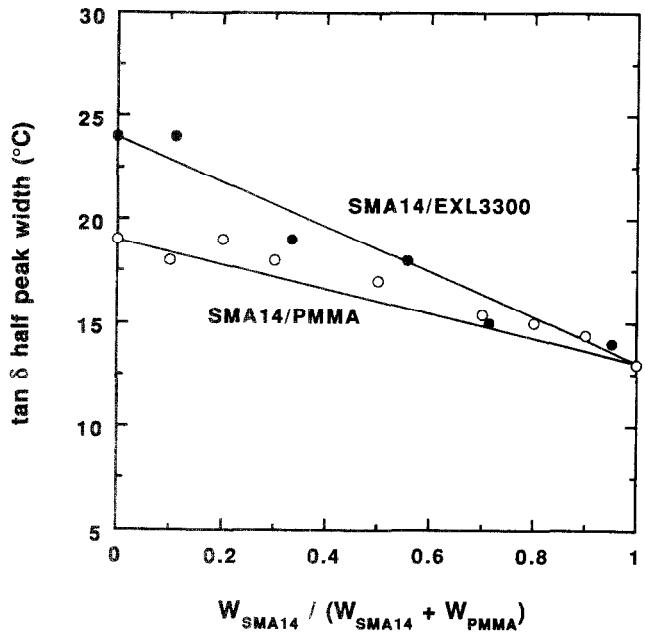

Figure 9 Width of the tan δ peak at half-height for the hard phase glass transition *versus* weight fraction of SMA14 in hard phase for SMA14/PMMA and SMA14/EXL3300 blends

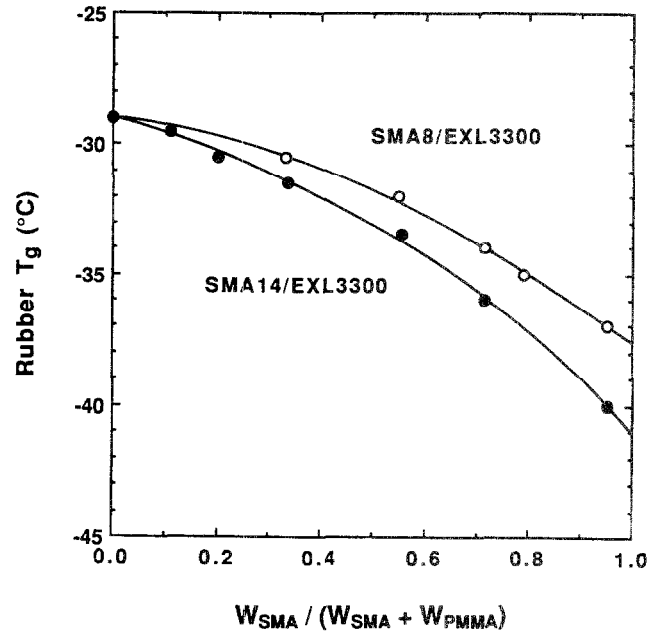

Figure 10 Glass transition temperature of rubber phase defined by the maximum of the tan δ curve for SMA/EXL3300 blends as function of weight fraction of SMA in hard phase

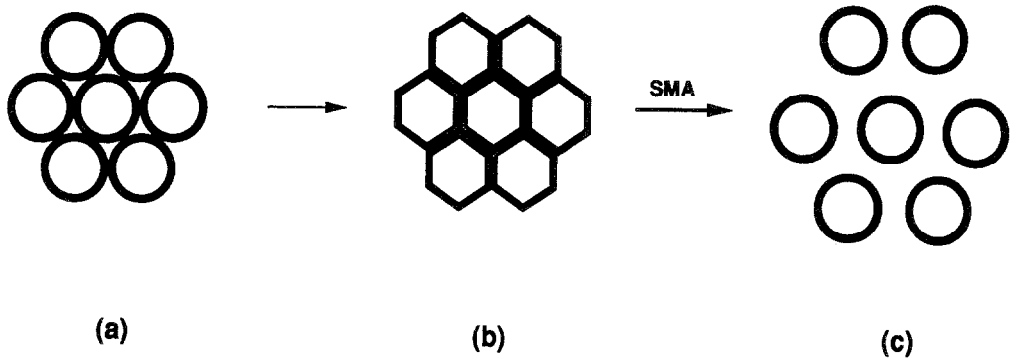

Figure 11 Schematic illustration of morphological changes that occur for blends of core–shell modifier particles as amount of SMA copolymer is increased

dense material unless the spherical particles deform. *Figure 11a* shows several such particles in a hexagonal close packing state without deformation; clearly there is space in the interstices that cannot be filled with polymer. Note that these drawings actually exaggerate by about two times the thickness of the shell relative to the particle diameter. If the particles deform into regular hexagons, then this packing problem is solved such that the shell material is now able to form a continuous phase by the chains grafted to the rubber core as illustrated in *Figure 11b*. Now if SMA copolymer is added, in a small amount relative to the total modifier content, then the continuous phase originally occupied by only shell material will expand; and the deformation of the spherical particles relaxes such that they return more towards their natural shape. This process is suggested by *Figure 11c*. Clearly if the amount of SMA8 added is great enough, the continuous phase must enlarge to a point where eventually the distance between particles is much larger than the dimensions of grafted chains, and uniform mixing of grafted chains in this space with the added polymer is not possible. That is, the SMA cannot be solubilized by the shell in unlimited amounts due to this geometrical constraint.

Blends of SMA8 with EXL3300 in varying proportions were examined by transmission electron microscopy using RuO_4 vapour to stain the SMA8 phase[33]; typical results are shown in *Figure 12*. No large aggregates of core–shell particles are observed for blends rich in SMA (e.g. *Figure 12c*) and there do not seem to be separate domains of SMA8 for blends rich in the impact modifier (e.g. *Figure 12a*). In *Figure 12* the dark phase is SMA8 and the light phase is the n-butyl acrylate rubber.

It would be useful for visualization purposes to stain the rubber core. Unfortunately, n-butyl acrylate rubber, the core of EXL3300, is not effectively stained by either RuO_4 or OsO_4[33]. Alternatively, a core–shell impact modifier containing a butadiene rubber core, EXL3607, was employed for this purpose. EXL3607 has a smaller

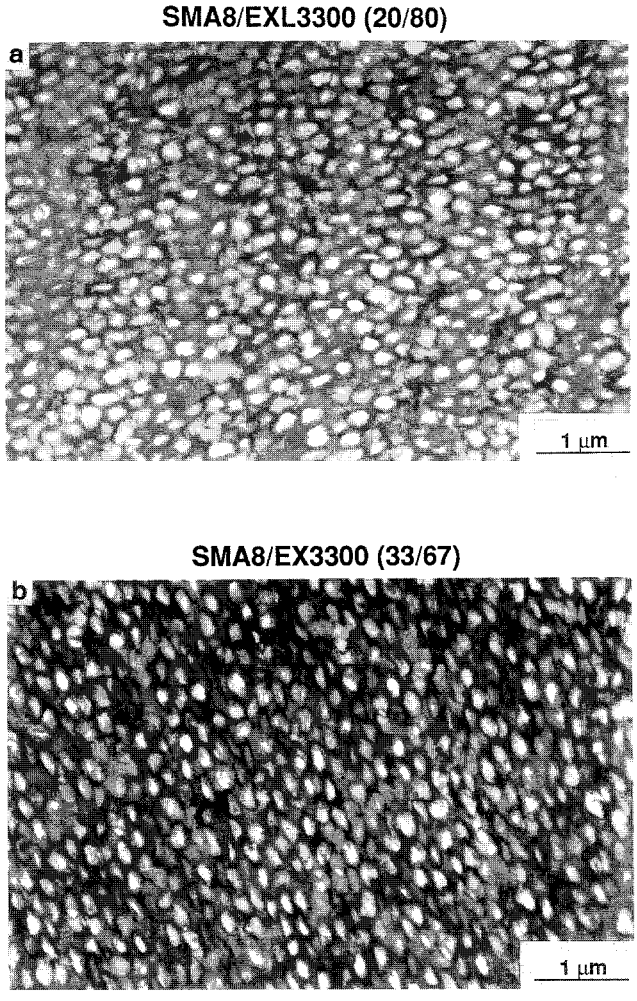

Figure 12 TEM photomicrographs of (a) 20/80 SMA8/EXL3300; (b) 33/67 SMA8/EXL3300; (c) 95/5 SMA8/EXL3300 blends. All the samples were cryogenically microtomed from compression moulded bars and stained with RuO_4

particle size than EXL3300 (0.18 *versus* 0.33 μm). *Figure 13* shows the morphological changes that occur as EXL3607 is blended with various amounts of SMA8. The specimens were stained by OsO_4 to render the rubber phase dark. For pure EXL3607, the core–shell particles are deformed from spheres into near hexagonal shapes, see *Figure 13a*, as suggested in *Figure 11b*. Adding only a small amount of SMA8 opens up the space between the particles to some extent but the shape of the rubber core remains hexagonal as shown in *Figure 13b*. The complex images seen here may reflect the fact that these thin microtomed sections (nominally 40 nm thick) may contain parts of some particles on top of parts of others. Further addition of SMA8 increases the space between these particles and the shape of the particles changes to spheres which are slightly elongated, possibly due to the shear flow during moulding or microtoming, see *Figures 13c* and *d*.

These TEM photomicrographs are consistent with a high degree of solubilization of SMA8 into the PMMA shells of EXL3300 and EXL3607; however, a quantitative determination of the upper limit of solubilization would be rather difficult. In fact, the following results suggest that such observations may not be taken as definitive proof of solubilization.

Polystyrene (PS), unlike these SMA copolymers, is not miscible with PMMA so a blend of PS with one of these core–shell impact modifiers might be expected to generate a different morphology in comparison to the blends shown in *Figures 12* and *13*. Unfortunately the glass transition temperatures of PMMA and PS are too close together to use this approach to examine the possibility of PS solubilization in the PMMA shell of core–shell impact modifiers. *Figure 14* shows a TEM photomicrograph of a 33/67 PS/EXL3607 blend stained by OsO_4 so that the butadiene rubber appears dark. The morphology seen in this case is not greatly different from that observed for SMA8 blends at the same composition (*Figures 12* and *13*). There is a hint of somewhat larger zones of unstained hard material in *Figure 14* that might be assumed to be PS domains, but even these regions are comparable in size to the emulsion particles. It should be recalled, however, that PS and PMMA have a very small, positive interaction energy[34] and, thus, are nearly miscible. The interfacial behaviour associated with such a small interaction energy combined with other factors, such as the rheological properties of each component and the processing conditions, contribute to the fine dispersion observed in these blends. Furthermore, it has been reported[35] that similar core–shell impact modifiers were readily dispersed in a PS matrix to a degree judged comparable to that when the matrix was a styrene/acrylonitrile copolymer containing 25% acrylonitrile, SAN25, which is miscible with PMMA. Therefore, the

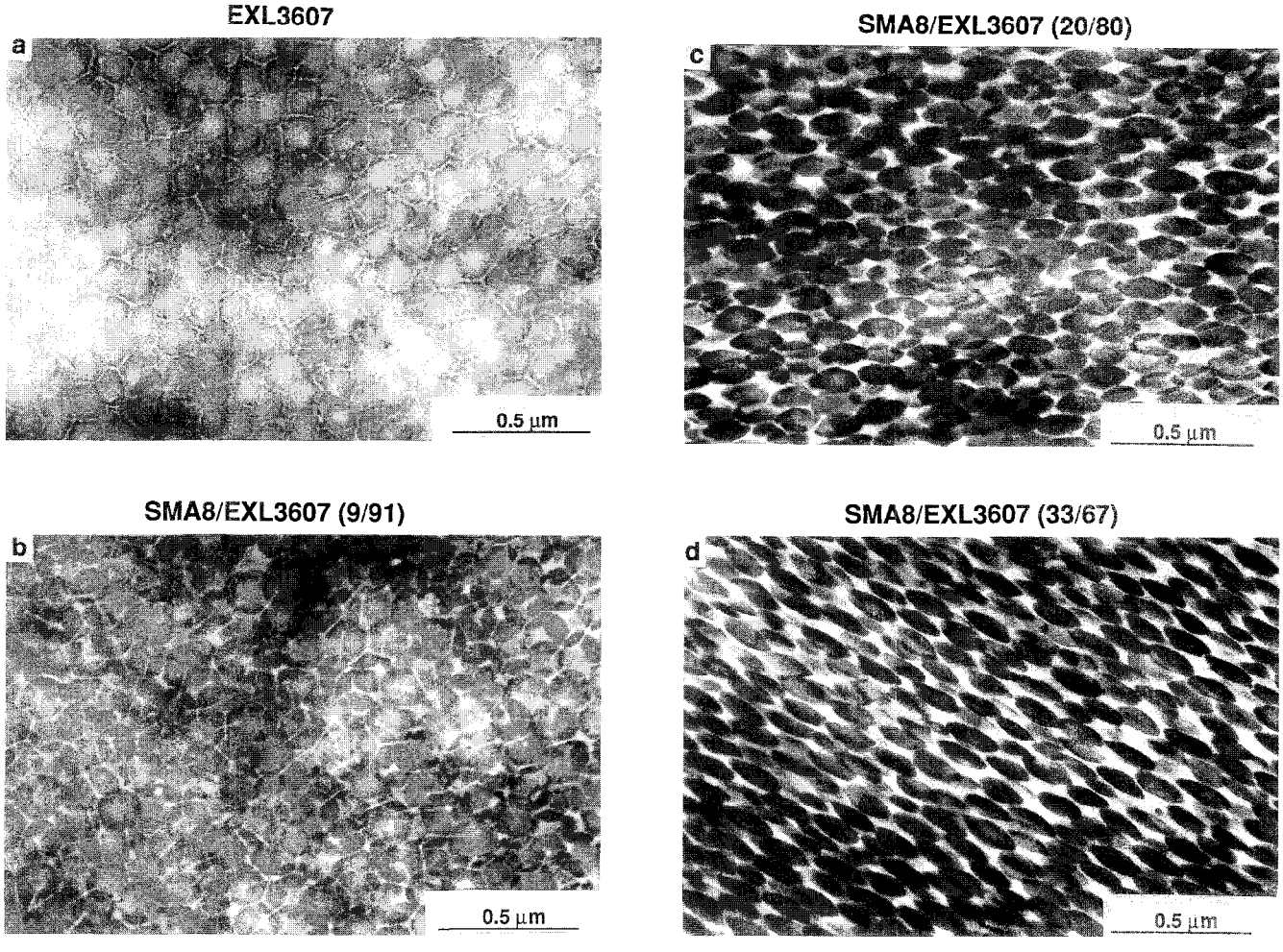

Figure 13 TEM photomicrographs of (a) EXL3607; (b) 9/91 SMA8/EXL3607; (c) 20/80 SMA8/EXL3607; (d) 33/67 SMA8/EXL3607 blends. All the samples were cryogenically microtomed from compression moulded bars and stained with OsO_4

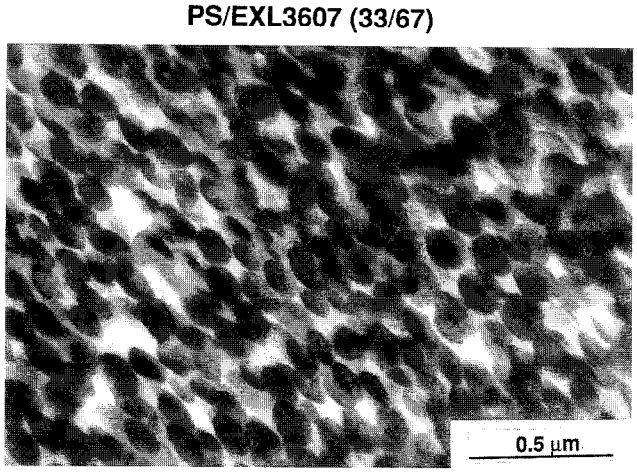

Figure 14 TEM photomicrograph of 33/67 PS/EXL 3607 blend. The sample was cryogenically microtomed from compression moulded bar and stained with OsO_4

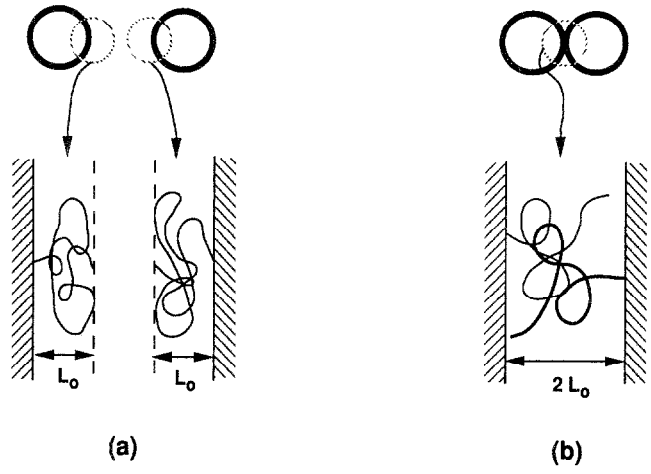

Figure 15 Schematic illustration of the conformations of grafted chains in the shell when the core–shell particles are isolated from one another (a) and when they are fused together (b)

apparent degree of dispersion of the core–shell particles alone cannot provide adequate evidence for solubilization, especially when the interaction between the shell and matrix is only weakly unfavourable. A matrix that has a more unfavourable interaction with the PMMA shell would no doubt show a quite different morphology for blends like these.

CONCLUSIONS

Styrene/maleic anyhdride copolymers containing 8 and 14% MA by weight are completely miscible with PMMA as revealed in previous studies[3] and shown here by the glass transition behaviour of these PMMA/SMA blends. One can expect these SMA copolymers to be solubilized in the PMMA shell of emulsion-made core–shell impact modifiers to a significant degree. This has been confirmed here by observations of the glass transition behaviour of blends of SMA8 and of SMA14 with such core–shell impact modifiers. Examination of the morphology of these blends by transmission electron microscopy techniques gives results consistent with this conclusion, but comparison experiments using polystyrene, which is not miscible with PMMA, rather than SMA copolymer reveal that this approach may not provide unambiguous evidence of solubilization.

There are at least two reasons why SMA copolymers should not be solubilized into the PMMA shell of these particles beyond some finite limit. First, the thermodynamic model described in the first paper of this series[1] indicates that conformational changes of both the PMMA grafted chains and the added SMA chains oppose their mixing and some balance must be reached with the favourable heat and entropy of mixing terms. This results in a finite upper solubilization limit which, based on the model in Part 1 of this series[1] and best estimates of the PMMA–SMA interaction energy, is of the order of 60–80% SMA in the shell for the materials of interest here. Second, simple geometrical issues suggest that mixing of large quantities of SMA into the PMMA graft or brush layer cannot occur (see *Figure 11*). That is, at an SMA content of the order of 90%, the PMMA chains are not long enough, even if fully extended, to extend to the outer limits of the swollen shell containing this amount of SMA.

It is important to point out here that the model described in Part 1 of this series[1] envisioned isolated core–shell particles, as they would exist when well dispersed in polyamide matrix[2]. In the current experiment, the particles are not isolated but are fused together (see *Figure 11*) during the melt process. These two states involve a subtle difference in the grafted chain conformation which can affect the thermodynamic analysis, as illustrated in *Figure 15*. In isolated particles, the grafted chain is limited to the shell region which has a thickness L_o. However, when particles agglomerate, chains grafted onto one particle can penetrate into the shell of adjacent particles, i.e. the space available is now $2L_o$. For low graft densities where the chains are 'compressed' into a shell thinner than is natural for a single chain, contact with other particles offers a new conformational degree of freedom which changes the thermodynamics of the solubilization process to some extent.

The current glass transition data do not reveal any well defined upper solubilization limit. In fact, cursory examination of the data would imply that there is one T_g even at very high SMA contents (see *Figures 6* and *7*). Indeed, very similar results have been seen for blends of poly(2,6-dimethyl-1,4-phenylene oxide) with styrene-based block copolymers[26,27,36,37] where analogous thermodynamic and geometrical constraints exist. To some extent, the glass transition technique is limited by sensitivity at the composition extremes. However, we do not believe this can be used as the sole explanation for such observations. It would be of considerable interest to examine mixing of polymers in constrained environments, e.g. graft layers and block copolymer microdomains, with a variety of techniques in order to reach a better understanding of all the issues and possibilities.

ACKNOWLEDGEMENTS

This research was sponsored by the US Army Research Office. The authors thank the Rohm and Haas Co. for donating the samples of core–shell impact modifiers.

REFERENCES

1 Lu, M. and Paul, D. R. *Polymer* 1996, **37**, 115

2 Lu, M., Keskkula, H. and Paul, D. R. *Polymer* 1993, **34**, 1874
3 Brannock, G. R., Barlow, J. W. and Paul, D. R. *J.Polym. Sci. Part B: Polym. Phys.* 1991, **29**, 413
4 Lu, M., Keskkula, H. and Paul, D. R. *J. Appl. Polym. Sci.* submitted
5 'Acryloid Impact Modifiers', Product Brochure MR-119, Rohm and Haas Co., 1984
6 Goldman, T. D. US Patent 4 443 585 (to Rohm and Haas Co.), 1984
7 Bohn, L. *Adv. Chem. Ser.* 1975, **142**, 66
8 Ricco, T., Pavan, A. and Danusso, F. *Polymer* 1975, **16**, 685
9 Krause, S. and Wang, B. *J.Polym. Sci., Polym. Lett. Edn* 1986, **24**, 35
10 Bates, F. E., Cohen, R. E. and Argon, A. S. *Macromolecules* 1983, **16**, 1108
11 Fox, T. G. *Bull. Am. Phys. Soc.* 1956, **2**, 123
12 Gordon, M. and Taylor, J. S. *J. Appl.Chem. USSR* 1952, **2**, 493
13 Jenckel, E. and Heusch, R. *Kolloid Z. 1953*, **130**, 89
14 Couchman, P. R. *Macromolecules* 1978, **11**, 1156
15 Couchman, P. R. *Phys. Lett.* 1979, **70A**, 155
16 Kewi, T. K. *J. Polym. Sci. Polym. Lett. Edn* 1984, **22**, 307
17 Lin, A. A., Kwei, T. K. and Reiser, A. *Macromolecules* 1989, **22**, 4112
18 Schneider, H. A. *Polymer* 1989, **30**, 771
19 Gordon, J. M., Rouse, B. G., Gibbs, J. H. and Risen, W. M. *J. Chem. Phys.* 1977, **60**, 4971
20 Couchman, P. R. and Karasz, F. E. *Macromolecules* 1978, **11**, 117
21 Brekner, M.-J., Schneider, H. A. and Cantow, H.-J. *Polymer* 1988, **29**, 78
22 Locke, C. E. and Paul, D. R. *Polym. Eng. Sci.* 1973, **13**, 308
23 Nielsen, L. 'Mechanical Properties of Polymers', Reinhold Publishing Co., New York, 1962
24 Dickie, R. A. in 'Polymer Blends' (Eds D. R. Paul and S. Newman), Academic Press, New York, 1978, Vol I, p. 370
25 MacKnight, W. J., Karasz, F. E. and Fried, J. R. in 'Polymer Blends' (Eds D. R. Paul and S. Newman), Academic Press, New York, 1978, Vol I, p. 226
26 Tucker, P. S., Barlow, J. W. and Paul, D. R. *J. Appl. Polym. Sci.* 1987, **34**, 1817
27 Tucker, P. S., Barlow, J. W. and Paul, D. R. *Macromolecules* 1988, **21**, 2794
28 Gan, P. P. and Paul, D. R. *J. Appl. Polym. Sci.* 1994, **54**, 317
29 Hobbs, S. Y., Dekkers, M. E. J. and Watkins, V. H. *Polymer* 1988, **29**, 1598
30 Hobbs, S. Y., Dekkers, M. E. J. and Watkins, V. H. *J. Mater. Sci.* 1988, **23**, 1219
31 Cheng, T. W., Keskkula, H. and Paul, D. R. *J. Appl. Polym. Sci.* 1992, **45**, 531
32 Brady, A. J., Keskkula, H. and Paul, D. R. *Polymer* 1994, **35**, 3665
33 Trent, J. S., Scheinbeim, J. I. and Couchman, P. R. *Macromolecules* 1983, **16**, 589
34 Callaghan, T. A. and Paul, D. R. *Macromolecules* 1993, **26**, 2439
35 Keskkula, H., Kim, H. and Paul, D. R. *Polym. Eng. Sci.* 1990, **30**, 1373
36 Tucker, P. S., Barlow, J. W. and Paul, D. R. *Macromolecules* 1988, **21**, 1678
37 Schultz, A. R. and Beach, B. M. *J. Appl. Polym. Sci.* 1977, **21**, 2305